Feasibility of quaternary ammonium and 1,4-diazabicyclo[2.2.2]octane-functionalized anion-exchange membranes for biohydrogen production in microbial electrolysis cells

René Cardeña[1], Jan Žitka[2], László Koók[3], Péter Bakonyi[3], Lukáš Pavlovec[2], Miroslav Otmar[2], Nándor Nemestóthy[3], Germán Buitrón[1,*]

[1] Laboratory for Research on Advanced Processes for Water Treatment, Instituto de Ingeniería, Unidad Académica Juriquilla, Universidad Nacional Autónoma de México, Blvd. Juriquilla 3001, Querétaro, Qro., México, 76230

[2] Institute of Macromolecular Chemistry, AS CR, Heyrovsky Sq. 2, 162 06 Prague 6, Czech Republic

[3] Research Institute on Bioengineering, Membrane Technology and Energetics, University of Pannonia, Egyetem ut 10, 8200 Veszprém, Hungary

*Corresponding author: Germán Buitrón

E-mail: gbuitronm@ii.unam.mx

Abstract

In this work, two commercialized anion-exchange membranes (AEMs), AMI-7001 and AF49R27, were applied in microbial electrolysis cells (MECs) and compared with a novel AEM (PSEBS CM DBC, functionalized with 1,4-diazabicyclo[2.2.2]octane) to produce biohydrogen. The evaluation regarding the effect of using different AEMs was carried out using simple (acetate) and complex (mixture of acetate, butyrate and propionate to mimic dark fermentation effluent) substrates. The MECs equipped with various AEMs were assessed based on their electrochemical efficiencies, H_2 generation capacities and the composition of anodic biofilm communities. pH imbalances, ionic losses and cathodic overpotentials were taken into consideration together with changes to substantial AEM properties (particularly ion-exchange capacity, ionic conductivity, area- and specific resistances) before and after AEMs were applied in the process to describe their potential impact on the behavior of MECs. It was concluded that the MECs which employed the PSEBS CM DBC membrane provided the highest H_2 yield and lowest internal losses compared to the two other separators. Therefore, it has the potential to improve MECs.

Keywords: microbial electrolysis cell; biohydrogen; anion-exchange membrane; volatile fatty acids; microbial community analysis; internal losses

1. Introduction

In bioelectrochemical technologies, e.g. microbial fuel cells (MFCs) [1-3], microbial synthesis cells (MSC) [4-5], microbial desalination cells (MDC) [6] and microbial electrohydrogenesis cells (MEC) [7-8], the system architecture, in particular the type and properties of the membrane separator applied between the electrode chambers, can play a notable role in terms of process performance [9-11]. The membrane, as a physical barrier, contributes to the adequate separation of anodic and cathodic reactions while allowing the required passage of ionic species, e.g. H^+ or OH^-, that maintain charge balancing and operation of the cell [12].

Researchers have shown, e.g. Harnisch and Schröder [13] and Sleutels et al. [14], that the transfer of H^+ or OH^- across an ion-exchange membrane (IEM) may be suppressed due to competition with other ions, namely sodium, potassium and calcium, present in relatively higher concentrations in the electrolyte solutions. Besides, the transport of both cations and anions other than H^+ or OH^- across a membrane can develop a pH gradient between the electrodes as well as unfavorable potential losses, which negatively affect the external energy demand of MECs needed to produce hydrogen gas [14]. To mitigate these side effects, a suitable IEM should be chosen. According to the findings by Sleutels et al. [14], MECs installed with AEMs may achieve higher operational efficiencies as a result of the more advantageous ratio of energy (voltage) input to membrane-associated energy losses. Experimental studies by Rozendal et al. [15-16], Cheng and Logan [17] and Ye and Logan [18] also proposed the deployment of AEM rather than CEM in MECs to reduce the imbalance in pH across the membrane and enhance the process. For example, the volumetric productivity of an MEC unit that employed an AEM was 2.1 L_{H2} L^{-1} d^{-1}, more than 5 times higher than the MEC that employed a CEM which attributed to the lower (internal) ion transport resistance of AEM-MEC [19]. Besides, in our recent work, a bioelectrochemical system (BES) in an MFC configured with PSEBS CM DBC AEM (polystyrene-block-poly(ethylene-ran-butylene)-block-polystyrene functionalized with 1,4-diazabicyclo[2.2.2]octane) notably outperformed those that employed either Nafion or AN-VPA 60 CEM [20], indicating the potential of this membrane material to improve microbial electrochemical technology. However, the PSEBS CM DBC AEM has been tested only in MFC-type BESs, where the current densities are generally moderate or low. Hence, it may be worth elaborating on the viability of this separator in applications that apply higher current densities and products other than electricity. In this way, more relevant feedback may be obtained regarding the potential of PSEBS CM DBC AEMs in various BESs. Driven by this motivation, to take a step forward and continue this proposed line of research, a comparative evaluation regarding the H_2 production capacities and electrochemical behavior of MECs in which PSEBS CM

DBC is applied was conducted with two commercialized AEMs, namely AMI-7001 and AF49R27 (MEGA, Czech Republic) as references. The comprehensive assessment of these MECs – fed either with a pure or mixed substrates (acetate vs. a mixture of volatile fatty acids (VFAs)) – was carried out by (i) evaluating the performance of the MEC (namely in terms of current density, H_2 production rate and yield, Coulombic efficiency and cathodic H_2 recovery), (ii) microbial community analysis of anodic biofilms and (iii) estimating pH-related as well as ionic voltage losses for the various AEMs. Moreover, all the membranes used were compared based on their operational stability. This is definitely a research gap as papers concerning changes to significant membrane properties before and after use in BESs are few and far between.

In accordance with the above, this work can provide new insights into the significance of membranes in MECs to produce H_2 with an increased degree of efficacy and enhance our understanding of the relationship between the behaviors of MECs and features of membranes.

2. Materials and Methods

2.1. Bioelectrochemical reactors

Two-chamber bioelectrochemical reactors (**Fig. 1**) made of acrylic were used with a working volume of 400 mL per chamber. The anode was composed of graphite felt (Brunssen de Occidente, S.A. de C.V.). The active surface area was approximately $9.3 \cdot 10^{-4}$ m^2 (by applying specifications from the supplier 129 cm^2 g^{-1}) and 0.006 m^2 for the projected area. The cathode was composed of nickel foam (5 cm x 5 cm, Sigma-Aldrich Corp., St. Louis, MO) with titanium wire acting as the current conductor. The membranes were located between the two chambers and the geometric surface area of the membranes was 5.5 cm x 5.5 cm. Neoprene seals were used to hold the membrane and tightly shut the reactor. The anode and cathode were placed at a distance of 0.5 cm and 0.9 cm from the membrane, respectively.

2.2. Anion-Exchange Membranes (AEM)

Three different AEMs were applied in the experiments. AMI-7001 (Membranes International Inc., Glen Rock, NJ) was pretreated at 40 °C in a 5 % NaCl solution for 24 h as recommended by the manufacturer. AF49R27 is a heterogeneous anion-exchange membrane (MEGA Inc., Czech Republic). PSEBS CM DBC is a homogenous anion-exchange membrane based on the block copolymer PSEBS (polystyrene-block-poly(ethylene-ran-butylene)-block-

polystyrene), functionalized with 1,4-diazabicyclo[2.2.2]octane and prepared according to Hnát et al. [21].

2.3. Membrane characterization

The properties of both pristine and used membranes were measured. The surface of each used membrane was first mechanically cleaned before the samples were conditioned as described in Section 2.3.1.

2.3.1. Ion-exchange capacity

The ion-exchange capacity (IEC) was determined twice for each membrane sample by titration [22-23]. The dry membrane samples (~0.5 g) were conditioned for 24 hours in a 1M NaOH solution before being washed with Q water to extract excess NaOH. By successively using HCl and NaOH, these steps were repeated twice to transform the AEMs into the OH^- form.

The samples of AEMs (~0.5 g) were dried at 35°C under a vacuum in Erlenmeyer flasks before their constant weights were measured. Subsequently, 15 mL of 4 % $NaNO_3$ solution was added to the dry samples, which were then shaken for 24 hours. 30 mL UV ethanol was added to 10 mL of this solution before extracting 2 mL from this sample to which 2 drops of 30 % $HClO_4$ and 3 drops of diphenylcarbazide (1 %) were added. Finally, the number of displaced chloride ions was titrated by 0.01 N $Hg(ClO_4)_2$. The color shift between light yellow and pink-violet indicated the end point of the titration.

2.3.2. Membrane resistance and ionic conductivity

Four-electrode impedance spectroscopy was applied to determine the resistance (R) of the membranes by using a potentiostat/galvanostat Metrohm Autolab PGSTAT302N, platinum working and Ag/AgCl reference electrodes [24-25]. Equilibrated membrane samples (of 14.5 mm in diameter) were placed between chambers of 25 mL in volume, which were filled with a 0.5 M KCl solution. The temperature of the system was kept constant at 25°C. During the measurements, a frequency range of $8 \cdot 10^5$ – 1 Hz and a current of 1 mA were applied. The area resistance ($R_A = R \cdot A$), specific resistance ($R_S = R_A \cdot L^{-1}$) and ionic conductivity ($\sigma = R_S^{-1}$) of each membrane were calculated with regard to the apparent surface area (A) and thickness (L) of the samples. The average thickness was derived from parallel measurements taken at multiple points on each membrane by an analog micrometer.

2.4. MEC start-up and operation

At start-up, by using 20 g of anaerobic granular sludge per liter (to treat wastewater from a beer factory in México) as the inoculum, the compartments of the MEC were flushed with N_2 gas to facilitate anaerobic conditions. The experiments were performed at 30 °C. The anodic and cathodic chambers were continuously mixed by using magnetic stirrers (175 rpm). The pH of the anolyte was initially set at 8 for each MEC cycle. A 125 mM NaCl solution was used as the catholyte without adjusting the pH [26-27]. From cycle to cycle throughout the experiments in this work, the anolyte and catholyte were replaced with a fresh medium/solution.

The colonization of the anode was followed by the determination of the current density profiles [28]. Graphite felt functioned as the working electrode (anode) and nickel foam as the counter electrode (cathode, place of hydrogen evolution) were separated by the membrane. The applied anode potential (E_{an}) was adjusted to +200 mV by a potentiostat/galvanostat VSP/Z-01 (Bio-Logic Science Instruments, France), which facilitates the enrichment of *Geobacter* spp*.* in electro-active biofilms [29-30]. All potential values are given against a Ag/AgCl reference electrode (3 M KCl, +210 mV against SHE, Radiometer Analytical SAS) placed in the anodic chamber.

MECs that applied the three membranes (AMI-7001, AF49R27, PSEBS CM DBC) were operated simultaneously. The fair reproducibility of each experiment under the influence of the same substrate loadings is reflected in the current density profiles (**Fig. 2**) [31], which seemed to be somewhat dependent on the membrane.

In total, an acclimation period of 40 days was ensured for the anodic biofilm formation to take place as follows. A week after inoculation, the MECs for all three membranes (AMI-7001, AF49R27, PSEBS CM DBC), which were fed repeatedly with 1 g_{COD} L^{-1} using acetate as a substrate, began producing current and by the 21st day, more or less similar current densities and hydrogen production capacities were observed. Stabilization of the reactors – interpreted as the initial colonization (biofilm formation) period – was noted after approximately one month of operation, therefore, further experiments using various pure and complex substrates were conducted as follows (evaluated in Section 3). At the end of the colonization stage (40 days), the anaerobic granular sludge (inoculum) was removed from the anode chambers of the MECs.

In the stabilized MECs (**Fig. 2**), the substrate in the anolyte was modified over two consecutive stages: (i) 1 g_{COD} L^{-1} using acetate as a substrate for the first stage and subsequently (ii) 1 g_{COD} L^{-1} in a mixture of volatile fatty acids (VFAs) (57 % butyrate, 30 % acetate and 13 % propionate to mimic the effluent of a dark fermentative H_2-producing bioreactor) was applied instead of just acetate. The proportion of VFAs was obtained based on a literature review of acidogenic

effluents produced from dark fermentation [32-38]. Regardless of the type of substrate, the MECs equipped with the various AEMs were kept running for at least 7 cycles. The operation time for each cycle was 24 hours. Overall, the experiments were conducted for 60 days, including 40 days to form the electroactive biofilm and 20 days to evaluate the substrates in terms of MEC performance using the three different AEMs.

Besides the actual substrate, throughout the entire MEC operation, each liter of anolyte was comprised of: 4.58 g Na_2HPO_4, 2.45 g $NaH_2PO_4 \cdot H_2O$, 0.31 g NH_4Cl, 0.13 g KCl, 12.5 mL of trace elements and 5 mL of vitamin solutions. Each liter of the solution of trace elements contained: 3.0 g $MgSO_4$, 0.5 g $MnSO_4 \cdot H_2O$, 1.0 g NaCl, 0.1 g $FeSO_4 \cdot 7H_2O$, 0.1 g $CaCl_2 \cdot 2H_2O$, 0.1 g $CoCl_2 \cdot 6H_2O$, 0.13 g $ZnCl_2$, 0.01 g $CuSO_4 \cdot 5H2O$, 0.01 g $AlK(SO_4)_2 \cdot 12H_2O$, 0.01 g H_3BO_3, 0.025 g Na_2MoO_4, 0.024 g $NiCl_2 \cdot 6H_2O$ and 0.025 g $Na_2WO_4 \cdot 2H_2O$. Each liter of the solution of vitamins contained: 10 mg pyridoxine, 5 mg p-Aminobenzoic acid, 5 mg nicotinic acid, 5 mg riboflavin, 5 mg thiamine, 2 mg biotin and 2 mg folic acid.

2.5. Analytical methods

The composition of the biogas (CH_4, CO_2, and H_2) was analyzed using a SRI 8610C gas chromatograph equipped with a thermal conductivity detector and a 30-m-long (0.53 mm ID) Carboxen-1010 PLOT column. The operating conditions were set as follows: the carrier gas was nitrogen at a flow rate of 4.5 mL/min; the temperature of the injector was 200 °C, the column was tempered at 100 °C and the temperature of the detector was fixed at 230 °C. The pH was measured at the starting point and endpoint of every batch by an Oakton pH meter. The Chemical Oxygen Demand (COD) was measured spectrophotometrically (using the Hach 435 and 430 methods). The volume of the biogas was measured by a displacement method using an inverted measuring cylinder filled with an acidified (pH=2) and saturated solution of NaCl.

2.6. Assessment of microbial populations

The microbial community analysis was carried out (i) at the end of the MEC operation with acetate (as a model substrate) and consecutively, and (ii) at the end of the experiment with the mixture of VFAs (mimicking a real substrate). First, the biofilm was scraped off the graphite felt anode, and the obtained biomass was further used to extract the bacterial genomic DNA using a DNeasy PowerSoil Pro Kit (QIAGEN, Carlsbad, CA) following the manufacturer's instructions. The resulting DNA was treated according to procedures described previously by Hernández et al. [39] in terms of the selection of markers, primers, amplification and Polymerase Chain Reaction (PCR) steps, reaction conditions, sequencing, as

well as bioinformatic and metagenomic tools. Besides anodic samples of MECs, the microbiological composition of the initial seed source was also determined.

2.7. Calculations

The electrochemical parameters were calculated at the end of every batch, the duration of each was 24 h. The projected surface of the anode was used to calculate the geometric current density (j / A m^{-2}) by assuming that during production the maximum current was sustained for a period of 4 h on average (I, in the unit of Ampers) in each batch cycle. The MEC performance was characterized by measures outlined in Eqs. 1-3 in accordance with Logan et al. [7].

Coulombic efficiency (C_E / %), Eq. 1:

$$C_E = \frac{\left(\int_{t-0}^{t} Idt\right) M_{O2}}{4F\Delta COD} \cdot 100 \quad (1)$$

where M_{O_2} denotes the molecular weight of oxygen (32 g mol^{-1}), F represents the Faraday constant (96,485 C mol^{-1} e^-), and ΔCOD (g) stands for the COD mass equivalent of substrate consumed.

Cathodic hydrogen recovery (r_{cat} / %), Eq. 2:

$$r_{cat} = \frac{2F\, n_{H2}}{\left(\int_{t-0}^{t} Idt\right)} \cdot 100 \quad (2)$$

where n_{H_2} denotes the actual moles of hydrogen gas recovered at the cathode.

For estimating the hydrogen yield (Y_{H2} / mL_{H2} g_{COD}^{-1}) Eq. 3 was employed:

$$Y_{H_2} = \frac{V_{H_2}}{\Delta COD} \quad (3)$$

where V_{H_2} denotes the amount of hydrogen produced (mL). The volumetric hydrogen production rate was calculated from the working volume of the cathode chamber and duration of the operating cycle (Q / mL_{H2} L_{cat}^{-1} d^{-1}).

3. Results and Discussion

3.1. Effects of membranes and substrates in stabilized MECs

3.1.1. Current densities and volumetric H_2 production rates

Chronoamperometric measurements were conducted to evaluate the time course of MEC performance using different AEMs and substrates (**Fig. 2**). AMI-7001 yielded the least stable current densities (**Fig. 2A**), while the MEC with AF49R27 exhibited the highest values with an increase in j within the last four batches of acetate (**Fig. 2B**). The PSEBS CM DBC membrane exhibited the most consistent current densities throughout the experiment (**Fig. 2C**) by and large independent from the type of substrate used. It was observed in general that the first cycle using the mixture of VFAs, regardless of the membrane applied, resulted in a drop in j, which, however, was temporary as the current density gradually recovered within all three MECs using the various AEMs.

The mean current densities achieved in the given MECs using acetate as a substrate are shown in **Fig. 3A**. As can be seen, among the 3 anion-exchange membranes, AF49R27 produced the highest mean current density (9.4 ± 0.9 A m^{-2}), while the lowest values were recorded using PSEBS CM DBC (6.4 ± 0.4 A m^{-2}). The change in substrate (from acetate to the mixture of VFAs) seemed to affect the current density in the MECs that used the membranes AMI-7001 (7.1 ± 1.9 A m^{-2}) and AF49R27 (7.4 ± 0.7 A m^{-2}), but not for MECs that employed the separator PSEBS CM DBC (**Fig. 3B**). The highest current densities achieved in the case of AF49R27 may be the result of the minimum resistance – in other words, maximum ionic conductivity – of this membrane (evaluated in Section 3.4 and summarized in **Table 2**).

Considering the fact that – in contrast to the membranes AMI-7001 and AF49R27 – the MEC equipped with PSEBS CM DBC was less sensitive to changes to the substrate, the nature of these membranes should be addressed. PSEBS CM DBC is a homogenous non-reinforced membrane prepared by solution casting and solvent evaporation from one kind of material. AF49R27 and AMI-7001 are heterogeneous membranes formed from a cross-linked ion-exchange resin dispersed in an inert polymer (AF49R27) and a reinforced cross-linked membrane (AMI-7001). Therefore, different ion transport kinetics are expected for various substrates in the case of homogeneous and heterogeneous membranes. Usually, homogeneous membranes are less affected by such changes. Overall, the aforementioned observations could be attributed to such basic differences between the membrane materials applied.

The values of j and Q obtained (**Fig. 3A**) exhibited similar tendencies when using acetate as a single substrate, indicating that electrons harvested at the

anode were used proportionally at the cathode to generate H_2 [7]. For the feed that consisted of a mixture of VFAs, in MECs that applied the membranes AF49R27 and PSEBS CM DBC, the values of Q decreased remarkably by 24 and 23 %, respectively (**Fig. 3B**).

In another work where the membrane Fumasep® FKE (FuMA-Tech GmbH, Germany) was applied, a productivity of 2.1 L_{H2} L^{-1} d^{-1}, and current density of 5.3 ± 0.5 A m^{-2} were obtained [14]. Besides, Carmona-Martínez et al. [28] achieved current densities of 10.6 A m^{-2} (199.1 A m^{-3}) and a maximum productivity of 0.9 L_{H2} L^{-1} d^{-1} in a tubular reactor using acetate (6.4 g L^{-1}) and AEM as a separator (FAA-PK, FuMA-Tech GmbH, Germany). Furthermore, Nam and Logan presented results similar to ours (current density of 131 ± 12 A m^{-2} and productivity of 1.6 ± 0.2 L_{H2} L^{-1} d^{-1}) by using the membrane AMI-7001 in MECs [26].

3.1.2. Hydrogen yield, Coulombic efficiency, cathodic hydrogen recovery and organic matter removal

The hydrogen yield facilitates the evaluation of MECs by correlating the H_2 produced based on the organic matter consumed. By taking into consideration the hydrogen yield produced by the MECs with different separators when acetate is the substrate (**Fig. 4**), the hierarchy of performance is as follows: PSEBS CM DBC (1117 ± 68 mL_{H2} g_{COD}^{-1}), AF49R27 (862 ± 108 mL_{H2} g_{COD}^{-1}) and AMI-7001 (847 ± 116 mL_{H2} g_{COD}^{-1}). The MEC assembled with the membrane PSEBS CM DBC produced the highest yield and represented approximately 79 % of the theoretical maximum yield (1419 mL_{H2} g_{COD}^{-1}) [7]. Changing the substrate from acetate to a VFA feedstock did not have a significant effect on the H_2 yield, irrespective of the membrane used.

In other studies, hydrogen yields of 1135 mL_{H2} g_{COD}^{-1} (AMI-7001) [26] and 1478 mL_{H2} g_{COD}^{-1} (Fumasep FAA AEM) [40] were accomplished using acetate and the acidic effluents of wastewater from fruit juice, respectively.

In terms of the C_E (**Fig. 5)**, no significant differences were recorded for the MECs operated using acetate as a substrate: AMI-7001 (69 ± 10 %) and AF49R27 (63 ± 3 %). Nevertheless, the best electron capture efficiency was associated with the application of PSEBS CM DBC (85 ± 6 %). Generally, the change in the type of substrate employed had little effect on the C_E. When evaluating the values concerning the removal of organic matter, a remarkable increase was observed in the case of the MEC equipped with AMI-7001 after switching the substrate from acetate to the VFA mixture (69 ± 4 % vs. 78 ± 2 %), while the other MECs exhibited similar levels of COD removal using both substrates.

By comparison, C_E in excess of 70 % was observed using an acidogenic effluent (composed of mainly acetate and butyrate) in an MEC that employed the membrane Fumasep FAA (FuMA-Tech BWT GmbH, Germany), moreover, COD

removal and r_{cat} of 72 % and 101 %, respectively were achieved using a Pt-Ir (90:10 %) cathode and applying a E_{an}= +0.2 V vs. SCE (saturated calomel electrode) [40]. However, the productivity did not exceed 25 mL_{H2} L^{-1} d^{-1} [40].

The r_{cat} is a variable that reflects the use of electrons harvested to form H_2 gas, which depends on certain architectural factors, e.g. the properties of the cathode material [41] (nickel foam in our study) as well as the current generated by the MECs under given operating conditions. Here, as seen in **Fig. 5**, r_{cat} was found to be rather independent of the actual AEM when both acetate and a VFA mixture were used as substrates. In the latter case, r_{cat} of the MECs that employed AMI-7001, AF49R27 and PSEBS CM DBC were 86 ± 3 %, 98 ± 2 % and 91 ± 4 %, respectively. The hydrogen purity recovered in the cathode chamber was > 95 % in all experiments. Additionally, only traces of carbon dioxide were detected in the cathode chamber.

In the study by Carmona-Martínez et al. [28], C_E and r_{cat} of 20-20 % in a 4 L MEC using the membrane FAA-PK (FuMA-Tech GmbH, Germany) were reported, which seem relatively lower compared to our aforementioned results. However, the rate of hydrogen production and the hydrogen purity were quite high, 900 mL_{H2} L^{-1} d^{-1} and > 90 %, respectively. Reactors of smaller volumes (28 mL and 30 mL for the anode and cathode chambers, respectively) that were equipped with AMI-7001, a graphite brush anode and a stainless steel cathode showed levels of organic matter removal of 90 %, r_{cat} of 117 % and C_E of 84 % [26].

3.2. Results of microbial community analysis

Since the set up of all MECs was identical, except for in terms of the membrane separator, the observed differences in their performances could have been related to the composition of the maturing microbial community in contact with the surface of the anode electrode [42].

The inoculum of MECs (anaerobic granular sludge) exhibited great microbial diversity, therefore, only the phylum level is presented in **Fig. 6A**. As can be seen, the inoculum was composed of *Proteobacteria* (21.91 %), *Thermotogae* (15.11 %), *Firmicutes* (7.6 %), *Cloacimonetes* (5.14 %), *Spirochaetes* (2.14 %), *Synergistetes* (1.86 %), *Bacteroidetes* (1.66 %) and *Nitrospirae* (0.61 %).

In samples of anodic biofilms from MECs that were analyzed at the end of the experiments which employed acetate as a substrate, the predominance of *Geobacter* spp. (84-94 %) was observed, according to **Figs. 6 B-D**. Consequently, it can be concluded that although the presence of *Geobacter* spp. in the seed source was initially marginal (0.0075 %), it was significantly enriched over time and became the leading microbial species on the anode when the 3 different kinds of membrane separators were employed. In bioelectrochemical systems, the predominance of *Geobacter* spp. in the anodic biofilm community suggests that

high current densities can be generated [43]. *Geobacter* spp. has been previously described as a microorganism capable of (i) oxidizing volatile fatty acids such as acetate and, hence (ii) producing electrons that are pumped extracellularly and harvested at the anode.

Moreover, it can be concluded from **Figs. 6 B-D** that by changing the substrate from pure acetate to a mixture of VFAs resulted in the additional selection of *Geobacter* spp. (95 – 97.5 %) and even lower levels of bacterial diversity for all membranes. Therefore, it would appear that by switching from a single to complex VFA feeding stream had a certain promoting impact and further supported the consistent growth of *Geobacter* spp. This can be of practical benefit when complex mixtures are loaded into and treated in the MEC, e.g. fermentation effluents comprised of remarkable quantities of VFAs [44].

It could be concluded from the aforementioned results that *Geobacter* spp. was the predominant genus which confirms that the new membrane material (PSEBS CM DBC) had no negative effect on the formation of the anodic electro-active biofilm. In fact, the anodes of MECs tended to contain similar species (meaning comparable microbial diversities), but it would appear that the MEC equipped with the membrane PSEBS CM DBC achieved a somewhat higher affinity for *Geobacter* spp.

3.3. Evaluation of the pH and ionic losses in MECs using different AEMs

In the case of MECs equipped with different separators, it is reasonable to assume that the characteristics of a particular membrane influence the pH balance on both sides of the membrane as well as the ionic composition of the anolyte and catholyte [45]. One of the main ideas behind proposing the use of AEMs instead of CEMs in BES is related to the theoretically more adequate management of the pH gradient that occurs between the cathode and anode chambers [14]. This pH imbalance inevitably leads to the loss of energy (voltage) ($E_{\Delta pH}$) in the MEC, which can be estimated according to Eq. 4 [19,46].

$$E_{\Delta pH} = \frac{RT}{F} \ln\left(10^{(pH_C - pH_A)}\right) \quad (4)$$

where pH_C and pH_A denote the mean pH values of the catholyte and anolyte, respectively, calculated as the mathematical average of the respective final pH values observed in the consecutive (individual) feeding cycles.

To evaluate the pH and ionic losses in the MECs, the potentials were determined after the start-up. The cathode potentials reported were measured in the stationary current-producing phase. In the case of acetate feedings, the mean final pH was 6.1 ± 0.2, 6.2 ± 0.2 and 6.3 ± 0.2 in the anolyte and 13 ± 0.1, 12.8 ±

0.1 and 12.5 ± 0.1 in the catholyte for AMI-7001-, AF49R27- and PSEBS CM DBC-equipped MECs, respectively. It seems that the pH shift was the lowest for PSEBS CM DBC and the highest for AMI-7001. Accordingly, the pH-related voltage drop followed the same order and fell to within the range of 373 – 415 mV (**Table 1**). In fact, the MEC that employed PSEBS CM DBC exhibited a $E_{\Delta pH}$ that was ~10 % less than that of the AMI-7001 equivalent.

In the cases where the VFA mixture was the substrate, similar conclusions can be made, however, the $E_{\Delta pH}$ values were somewhat smaller in each MEC. In addition, the difference between the highest (AMI-7001) and lowest (PSEBS CM DBC) $E_{\Delta pH}$ decreased by ~7.5 %. Thus, it could be observed that the pH splitting effect was notable and varied depending on the type of membrane employed. In conclusion, the membrane PSEBS CM DBC demonstrated the most beneficial features from this point of view.

In terms of electrolyte resistance (associated with the ionic composition and thus, the conductivity of the solution), the ionic voltage drop (E_{ionic}) could be dependent on the flow of ions (current density, j), the membrane-anode and membrane-cathode distances (d_A and d_C, respectively), as well as the conductivities of the anolyte and catholyte (κ_A and κ_C, respectively), as expounded in Eq. 5 [47]:

$$E_{ionic} = j\left(\frac{d_A}{\kappa_A} + \frac{d_C}{\kappa_C}\right) \quad (5)$$

As listed in **Table 1**, the MEC equipped with the membrane AF49R27 exhibited the highest E_{ionic} with both acetate and a mixture of VFAs as substrates. In general, E_{ionic} was one order of magnitude lower than $E_{\Delta pH}$, indicating the dominance of pH-related losses over those linked to ionic compounds of electrolytes in the MECs [15-16].

To further evaluate the potential losses in the different MECs and support the aforementioned data concerning $E_{\Delta pH}$ and E_{ionic}, the cathodic overpotentials can also be taken into consideration. It was observed that in the case of both feedings using acetate and a mixture of VFAs, the system equipped with PSEBS CM DBC exhibited by far the lowest cathodic overpotentials (**Table 1**). So far in this study, it has been demonstrated that PSEBS CM DBC could be less sensitive to changes in substrate that would appear to be a consequence of its homogeneous polymer nature (and concomitantly different ion-transfer kinetics) (Section 3.1). Furthermore, this membrane ensured efficient operation of the MEC based on the reduction of losses related to pH imbalance and the change in the ionic composition of the electrolytes in the MEC. Therefore, given all these aspects, the use of PSEBS CM DBC resulted in a lower cathodic overpotential for the hydrogen evolution reaction in the MEC, when compared to the commercial, heterogeneous

AEMs tested. These relatively advantageous features indicate the notable potential of applying the membrane PSEBS CM DBC in MECs. In the next section, the membranes and, in particular, their stability will be evaluated by the intrinsic material properties and their alteration over the course of operation of MECs.

3.4. Assessment of membrane stability in MECs

The operating efficacy of BESs may be affected by changes to the properties of membrane separators over time, e.g. due to (bio)fouling [3,10]. Therefore, especially when new membrane materials such as AF49R27 and PSEBS CM DBC are tested in BESs, it is crucial to check their in-use stabilities compared to ones that have already been commercialized, e.g. AMI-7001 in this research.

During our experiments, the three membranes tested were exposed to significant pH gradients (pH 6.2–6.9, as presented in Section 3.3) that developed between the anode and cathode chambers. The stability of AEMs in an alkaline environment might be problematic [48-49], and since the final pH of the catholyte exceeded 12 in all the MECs, it appeared to be important to gain insights into the possible alteration of membrane traits and evaluate them in the light of those of unused materials. These measured characteristics (R_A, R_S, σ, IEC and L) are summarized in **Table 2**.

AMI-7001 exhibited the highest area specific resistance but the lowest ionic conductivity, followed by PSEBS CM DBC and AF49R27, for both the pristine and used materials. For example, the ionic conductivity of the unused AMI-7001 was 3.97 times and 2.16 times lower than that of both AF49R27 and PSEBS CM DBC, respectively. Furthermore, concerning IEC – which provides information about the amount of active functional groups on the given membrane material [23] – it turned out (as expected) that AF49R27 exhibited a remarkably higher IEC than AMI-7001 in both pristine and used states (45.5 % and 40.4 %, respectively). This observation, keeping in mind that the membrane AF49R27 was considerably thinner (almost half as thick as AMI-7001), is a result of the higher ionic conductivity and underlines the potential benefit of applying AF49R27 over AMI-7001 in MECs. In the case of PSEBS CM DBC, however, the IEC appeared to be lower compared to that of AMI-7001 (0.77 vs. 1.32 meq. g^{-1} for pristine and 0.81 vs. 1.31 meq g^{-1} for used samples, respectively). Nonetheless, given that the pristine and used samples were 53 % and 49 % thinner when compared to the AMI-7001 equivalents, respectively, a higher ionic conductivity of PSEBS CM DBC can be presumed.

Alterations to the aforementioned features of the membrane as a result of use in MECs are displayed in **Fig. 7**. First of all, it can be inferred that in the case of AMI-7001, alterations to all terms fell within the range of methodological

accuracy, which is indicative of an excellent degree of durability (a desirable characteristic for a widely applied commercial material) in such complex and dynamic environments as those found in MECs. Moreover, the outcomes suggest the in-use stability of the other two membranes as well since alterations of less than 10 % were observed (except for R_A in the case of PSEBS CM DBC, where it was 12 %). During the operation of MECs, the thickness of the membrane PSEBS CM DBC changed the most, while it remained rather comparable for the other two materials before and after being used. AF49R27 suffered from the largest reduction in ionic conductivity, although after use it still exhibited the highest ionic conductivity of all three AEMs. The IEC seemed to be stable in all cases (alterations were of less than 5 %), implying the remarkable chemical stability of the investigated polymers. This can be seen as a factor when new membranes, e.g. PSEBS CM DBC, are benchmarked [50-51].

In conclusion, PSEBS CM DBC as a novel separator for use in MECs seems more technologically feasible compared to AMI-7001, making it a potential alternative membrane to be deployed in MECs.

4. Conclusions

In this work, a novel anion-exchange membrane, PSEBS CM DBC (functionalized with 1,4-diazabicyclo[2.2.2]octane), was compared with quaternary ammonium-functionalized, commercially available AEMs, namely AMI-7001 and AF49R27, in terms of producing hydrogen gas in MECs. Given the outcomes of research where acetate or a mixture of VFAs were applied as substrates, PSEBS CM DBC could be more suitable for MECs than the two other membranes when H_2 production data, electrochemical behavior, as well as microbiological insights into anodic populations and internal losses are all taken into consideration. Moreover, analysis of the alterations of various membrane properties following their use in MECs indicated that PSEBS CM DBC was sufficiently stable when compared to commercialized materials, making it a promising candidate for sustainable MEC operation.

Acknowledgements

This research was supported through Fondo de Sustentabilidad Energética SENER-CONACYT [grant number 247006 Gaseous Biofuels Cluster]. The authors are grateful to Sarai E. Rodríguez, Jaime Perez and Gloria Moreno for the technical support and fruitful discussions. Péter Bakonyi acknowledges the support received from National Research, Development and Innovation Office (Hungary) [grant number PD 115640]. László Koók was supported by the ÚNKP-19-3 New National Excellence Program of the Ministry for Innovation and Technology.

References

[1] B.E. Logan, B. Hamelers, R. Rozendal, U. Schröder, J. Keller, S. Freguia et al., Microbial fuel cells: methodology and technology, Environ. Sci. Technol. 40 (2006) 5181-5192. https://doi.org/10.1021/es0605016

[2] C. Santoro, C. Arbizzani, B. Erable, I. Ieropoulos, Microbial fuel cells: From fundamentals to applications. A review, J. Power Sources 356 (2017) 225-244. https://doi.org/10.1016/j.jpowsour.2017.03.109

[3] P. Bakonyi, L. Koók, G. Kumar, G. Tóth, T. Rózsenberszki, D.D. Nguyen et al., Architectural engineering of bioelectrochemical systems from the perspective of polymeric membrane separators: A comprehensive update on recent progress and future prospects, J. Membr. Sci. 564 (2018) 508-522. https://doi.org/10.1016/j.memsci.2018.07.051

[4] S. Bajracharya, S. Srikanth, G. Mohanakrishna, R. Zacharia, D.P. Strik, D. Pant, Biotransformation of carbon dioxide in bioelectrochemical systems: State of the art and future prospects, J. Power Sources 356 (2017) 256-273. https://doi.org/10.1016/j.jpowsour.2017.04.024

[5] S. Gildemyn, K. Verbeeck, R. Jansen, K. Rabaey, The type of ion selective membrane determines stability and production levels of microbial electrosynthesis, Bioresour. Technol. 224 (2017) 358-364. https://doi.org/10.1016/j.biortech.2016.11.088

[6] E. Yang, K.J. Chae, M.J. Cho, Z. He, I.S. Kim, Critical review of bioelectrochemical systems integrated with membrane based technologies for desalination, energy self-sufficiency, and high efficiency water and wastewater treatment, Desalination 452 (2019) 40-67. https://doi.org/10.1016/j.desal.2018.11.007

[7] B.E. Logan, D. Call, S. Cheng, H.V.M. Hamelers, T.H.J.A. Sleutels, A.W. Jeremiasse et al., Microbial electrolysis cells for high yield hydrogen gas production from organic matter, Environ. Sci. Technol. 42 (2008) 8630-8640. https://doi.org/10.1021/es801553z

[8] G. Zhen, X. Lu, G. Kumar, P. Bakonyi, X. Kaiqin, Z. Youcai, Microbial electrolysis cell platform for simultaneous waste biorefinery and clean electrofuels generation: Current situation, challenges and future perspectives, Prog. Energy Combust. Sci. 63 (2017) 119-145. https://doi.org/10.1016/j.pecs.2017.07.003

[9] S.A. Patil, S. Gildemyn, D. Pant, K. Zengler, B.E. Logan, K. Rabaey, A logical data representation framework for electricity-driven bioproduction processes, Biotechnol. Adv. 33 (2015) 736-744. https://doi.org/10.1016/j.biotechadv.2015.03.002

[10] L. Koók, P. Bakonyi, F. Harnisch, J. Kretzschmar, K.J. Chae, G. Zhen et al., Biofouling of membranes in microbial electrochemical

technologies: Causes, characterization methods and mitigation strategies, Bioresour. Technol. 279 (2019) 327-338. https://doi.org/10.1016/j.biortech.2019.02.001

[11] M.T. Noori, M.M. Ghangrekar, C.K. Mukherjee, B. Min, Biofouling effects on the performance of microbial fuel cells and recent advances in biotechnological and chemical strategies for mitigation, Biotechnol. Adv. (2019) 107420, https://doi.org/10.1016/j.biotechadv.2019.107420

[12] F. Harnisch, R. Warmbier, R. Schneider, U. Schröder, Modeling the ion transfer and polarization of ion exchange membranes in bioelectrochemical systems, Bioelectrochemistry 75 (2009) 136-141. https://doi.org/10.1016/j.bioelechem.2009.03.001

[13] F. Harnisch, U. Schröder, Selectivity versus Mobility: Separation of Anode and Cathode in Microbial Bioelectrochemical Systems, ChemSusChem 2 (2009) 921-926. https://doi.org/10.1002/cssc.200900111

[14] T.H.J.A. Sleutels, A. ter Heijne, P. Kuntke, C.J.N. Buisman, H.V.M. Hamelers, Membrane selectivity determines energetic losses for ion transport in bioelectrochemical systems, ChemistrySelect 2 (2017) 3462-3470. https://doi.org/10.1002/slct.201700064

[15] R.A. Rozendal, H.V.M. Hamelers, R.J. Molenkamp, C.J.N. Buisman, Performance of single chamber biocatalyzed electrolysis with different types of ion exchange membranes, Water Res. 41 (2007) 1984-1994. https://doi.org/10.1016/j.watres.2007.01.019

[16] R.A. Rozendal, T.H.J.A. Sleutels, H.V.M. Hamelers, C.J.N. Buisman, Effect of the type of ion exchange membrane on performance, ion transport, and pH in biocatalyzed electrolysis of wastewater, Water Sci. Technol. 57 (2008) 1757-1762. https://doi.org/10.2166/wst.2008.043

[17] S. Cheng, B.E. Logan, Evaluation of catalysts and membranes for high yield biohydrogen production via electrohydrogenesis in microbial electrolysis cells (MECs), Water Sci. Technol. 58 (2008) 853-857. https://doi.org/10.2166/wst.2008.617

[18] Y. Ye, B.E. Logan, The importance of OH^- transport through anion exchange membrane in microbial electrolysis cells, Int. J. Hydrogen Energy 43 (2018) 2645-2653. https://doi.org/10.1016/j.ijhydene.2017.12.074

[19] T.H.J.A. Sleutels, H.V.M. Hamelers, R.A. Rozendal, C.J.N. Buisman, Ion transport resistance in Microbial Electrolysis Cells with anion and cation exchange membranes, Int. J. Hydrogen Energy 34 (2009) 3612-3620. https://doi.org/10.1016/j.ijhydene.2009.03.004

[20] L. Koók, E.D.L. Quéméner, P. Bakonyi, J. Zitka, E. Trably, G. Tóth et al., Behavior of two-chamber microbial electrochemical systems started-up with different ion-exchange membrane separators, Bioresour. Technol. 278 (2019) 279-286. https://doi.org/10.1016/j.biortech.2019.01.097

[21] J. Hnát, M. Plevová, J. Zitka, M. Paidar, K. Bouzek, Anion-selective materials with 1,4-diazabicyclo[2.2.2]octane functional groups for advanced alkaline water electrolysis, Electrochim. Acta 248 (2017) 547-555. https://doi.org/10.1016/j.electacta.2017.07.165.

[22] H. Strathmann, Ion-exchange membrane separation processes (Vol. 9), Elsevier, 2004.

[23] Y. Tanaka, Ion Exchange Membranes: Fundamentals and Applications, Series 12, Membrane Science and Technology: Elsevier, Netherlands, 2007.

[24] J. Schauer, V. Kůdela, K. Richau, R. Mohr, Heterogeneous ion-exchange membranes based on sulfonated poly(1,4-phenylene sulfide), Desalination 198 (2006) 256-264. https://doi.org/10.1016/j.desal.2005.12.027

[25] J. Schauer, J. Hnát, L. Brožová, J. Žitka, K. Bouzek, Heterogeneous anion-selective membranes: Influence of a water-soluble component in the membrane on the morphology and ionic conductivity, J. Membr. Sci. 401 (2012) 83-88. https://doi.org/10.1016/j.memsci.2012.01.038

[26] J.Y. Nam, B.E. Logan, Enhanced hydrogen generation using a saline catholyte in a two chamber microbial electrolysis cell, Int. J. Hydrogen Energy 36 (2011) 15105-15110. https://doi.org/10.1016/j.ijhydene.2011.08.106

[27] Y. Ahn, B.E. Logan, Saline catholytes as alternatives to phosphate buffers in microbial fuel cells, Bioresour. Technol. 132 (2013) 436-439. https://doi.org/10.1016/j.biortech.2013.01.113

[28] A.A. Carmona-Martínez, E. Trably, K. Milferstedt, R. Lacroix, L. Etcheverry, N. Bernet, Long-term continuous operation of H_2 in microbial electrolysis cell (MEC) treating saline wastewater, Water Res. 81 (2015) 149-156. https://doi.org/10.1016/j.watres.2015.05.041

[29] B.H. Kim, H.S. Park, H.J. Kim, G.T. Kim, I.S. Chang, J. Lee et al., Enrichment of microbial community generating electricity using a fuel-cell-type electrochemical cell, Appl. Microbiol. Biotechnol. 63 (2004) 672-681. https://doi.org/10.1007/s00253-003-1412-6

[30] Y. Liu, F. Harnisch, K. Fricke, R. Sietmann, U. Schröder, Improvement of the anodic bioelectrocatalytic activity of mixed culture biofilms by a simple consecutive electrochemical selection procedure, Biosens. Bioelectron. 24 (2008) 1006-1011. https://doi.org/10.1016/j.bios.2008.08.001

[31] S. Mateo, P. Cañizares, M.A. Rodrigo, F.J. Fernández-Morales, Reproducibility and robustness of microbial fuel cells technology, J. Power Sources 412 (2019) 640-647. https://doi.org/10.1016/j.jpowsour.2018.12.007

[32] J.I. Horiuchi, T. Shimizu, K. Tada, T. Kanno, M. Kobayashi, Selective production of organic acids in anaerobic acid reactor by pH control, Bioresour. Technol. 82 (2002) 209-213. https://doi.org/10.1016/S0960-8524(01)00195-X

[33] S.K. Khanal, W.H. Chen, L. Li, S. Sung, Biological hydrogen production: effects of pH and intermediate products, Int. J. Hydrogen Energy 29 (2004) 1123-1131. https://doi.org/10.1016/j.ijhydene.2003.11.002

[34] I. Hussy, F.R. Hawkes, R. Dinsdale, D.L. Hawkes, Continuous fermentative hydrogen production from sucrose and sugarbeet, Int. J. Hydrogen Energy 30 (2005) 471-483. https://doi.org/10.1016/j.ijhydene.2004.04.003

[35] C.Y. Lin, C.H. Lay, A nutrient formulation for fermentative hydrogen production using anaerobic sewage sludge microflora, Int. J. Hydrogen Energy 30 (2005) 285-292. https://doi.org/10.1016/j.ijhydene.2004.03.002

[36] H.N. Gavala, I.V. Skiadas, B.K. Ahring, Biological hydrogen production in suspended and attached growth anaerobic reactor systems, Int. J. Hydrogen Energy, 31 (2006) 1164-1175. https://doi.org/10.1016/j.ijhydene.2005.09.009

[37] N. Ren, J. Li, B. Li, Y. Wang, S. Liu, Biohydrogen production from molasses by anaerobic fermentation with a pilot-scale bioreactor system, Int. J. Hydrogen Energy, 31 (2006) 2147-2157. https://doi.org/10.1016/j.ijhydene.2006.02.011

[38] Y. Tao, Y. Chen, Y. Wu, Y. He, Z. Zhou, High hydrogen yield from a two-step process of dark- and photo-fermentation of sucrose, Int. J. Hydrogen Energy 32 (2007) 200-206. https://doi.org/10.1016/j.ijhydene.2006.06.034

[39] C. Hernández, Z.L. Alamilla-Ortiz, A.E. Escalante, M. Navarro-Díaz, J. Carrillo-Reyes, I. Moreno-Andrade et al., Heat-shock treatment applied to inocula for H_2 production decreases microbial diversities, interspecific interactions and performance using cellulose as substrate, Int. J. Hydrogen Energy 44 (2019) 13126-13134. https://doi.org/10.1016/j.ijhydene.2019.03.124

[40] A. Marone, O.R. Ayala-Campos, E. Trably, A.A. Carmona-Martínez, R. Moscoviz, E. Latrille et al., Coupling dark fermentation and microbial electrolysis to enhance bio-hydrogen production from agro-industrial wastewaters and by-products in a bio-refinery framework, Int. J. Hydrogen Energy 42 (2017) 1609-1621. https://doi.org/10.1016/j.ijhydene.2016.09.166

[41] A. Kundu, J.N. Sahu, G. Redzwan, M.A. Hashim, An overview of cathode material and catalysts suitable for generating hydrogen in microbial electrolysis cell, Int. J. Hydrogen Energy 38 (2013) 1745-1757. https://doi.org/10.1016/j.ijhydene.2012.11.031

[42] C.I. Torres, A.K. Marcus, H.S. Lee, P. Parameswaran, R. Krajmalnik-Brown, B.E. Rittmann, A kinetic perspective on extracellular electron transfer by anode-respiring bacteria, FEMS Microbiol. Rev. 34 (2010) 3-17. https://doi.org/10.1111/j.1574-6976.2009.00191.x

[43] P. Chatterjee, P. Dessi, M. Kokko, A.M. Lakaniemi, P. Lens, Selective enrichment of biocatalysts for bioelectrochemical systems: A critical review, Renew. Sustain. Energy Rev. 109 (2019) 10-23. https://doi.org/10.1016/j.rser.2019.04.012

[44] P. Bakonyi, G. Kumar, L. Koók, G. Tóth, T. Rózsenberszki, K. Bélafi-Bakó et al., Microbial electrohydrogenesis linked to dark fermentation as integrated application for enhanced biohydrogen production: a review on process characteristics, experiences and lessons, Bioresour. Technol. 251 (2018) 381-389. https://doi.org/10.1016/j.biortech.2017.12.064

[45] M. Oliot, S. Galier, H. Roux de Balmann, A. Bergel, Ion transport in microbial fuel cells: Key roles, theory and critical review, Appl. Energy 183 (2016) 1682-1704. https://doi.org/10.1016/j.apenergy.2016.09.043

[46] R.A. Rozendal, H.V.M. Hamelers, C.J.N. Buisman, Effects of membrane cation transport on pH and microbial fuel cell performance, Environ. Sci. Technol. 40 (2006) 5206-5211. https://doi.org/10.1021/es060387r

[47] A. Ter Heijne, H.V.M. Hamelers, V. De Wilde, R.A. Rozendal, C.J.N. Buisman, A bipolar membrane combined with ferric iron reduction as an efficient cathode system in microbial fuel cells, Environ. Sci. Technol. 40 (2016) 5200-5205. https://doi.org/10.1021/es0608545

[48] B. Bauer, H. Strathmann, F. Effenberger, Anion-exchange membranes with improved alkaline stability, Desalination 79 (1990) 125-144. https://doi.org/10.1016/0011-9164(90)85002-R

[49] M.A. Hickner, A.M. Herring, E.B. Coughlin, Anion exchange membranes: Current status and moving forward, J. Polym. Sci. Pol. Phys. 51 (2013) 1727-1735. https://doi.org/10.1002/polb.23395

[50] G.G. Scherer, Polymer membranes for fuel cells, Ber. Bunsenges. Physik. Chem. 94 (1990) 1008-1014. https://doi.org/10.1002/bbpc.19900940926

[51] E.N. Komkova, D.F. Stamatialis, H. Strathmann, M. Wessling, Anion-exchange membranes containing diamines: preparation and stability in alkaline solution, J. Membr. Sci. 244 (2004) 25-34. https://doi.org/10.1016/j.memsci.2004.06.026

Figure Legends

Fig. 1 – The MEC setup used in this work

Fig. 2 – Chronoamperometry of the MECs with different AEMs: A) AMI-7001, B) AF49R27 and C) PSEBS CM DBC

Fig. 3 – Current density and H_2 production rate of two-chamber MECs with different AEMs. A) Substrate: acetate; B) Substrate: VFA mixture

Fig. 4 – Performance (hydrogen yield) of two-chamber MECs with different AEMs

Fig. 5 – Coulombic efficiency (C_E), cathodic hydrogen recovery (r_{cat}) and organic matter removal of two-chamber MEC operated with various AEMs

Fig. 6 – A) Relative abundance in the microbial communities for the inoculum (phylum level). Relative abundance for the genus level in the microbial communities present in anode biofilms using: B) AMI-7001 C) AF49R27 and D) PSEBS CM DBC.

Fig. 7 – Alterations in membrane properties before and after use in MEC

789 Table 1 – Cathode potentials and various losses of MECs

790

	PSEBS CM DBC	AF49R27	AMI - 7001
$E_{\Delta pH}$ / mV, Acetate	373 ± 11	397 ± 12	415 ± 12
$E_{\Delta pH}$ / mV, Ac/Prop/But	367 ± 6	373 ± 6	397 ± 12
E_{ionic} / mV, Acetate	23.7 ± 1.5	36.0 ± 3.5	27.0 ± 3.3
E_{ionic} / mV, Ac/Prop/But	25.0 ± 2.5	28.0 ± 2.8	24.2 ± 9.1
E_{cat} / mV vs. Ag/AgCl, Acetate	-834 ± 31	-934 ± 73	-1291 ± 56
E_{cat} / mV vs. Ag/AgCl, Ac/Prop/But	-785 ± 24	-921 ± 27	-1362 ± 67

791 Abbreviations: $E_{\Delta pH}$ – Energy loss due to pH imbalance; E_{ionic} – Ionic voltage loss; E_{cat} –
792 Cathode potential; Ac/Prop/But – Mixture of VFAs containing acetate, propionate and
793 butyrate

794 Table 2 – Main properties of pristine and used anion exchange membranes

795

	PSEBS CM DBC		AF49 R27		AMI - 7001	
Property	Pristine	Used	Pristine	Used	Pristine	Used
R_A / Ω cm^2	2.96 ± 0.08	3.31 ± 0.2	1.66 ± 0.14	1.81 ± 0.13	13.72 ± 0.31	13.29 ± 0.28
R_S / Ω cm	117.7 ± 3.9	124 ± 3.5	64.4 ± 5.2	71.2 ± 5.0	254.9 ± 7.3	250.9 ± 4.2
σ / mS cm^{-1}	8.51 ± 0.28	8.07 ± 0.23	15.62 ± 1.36	14.09 ± 1.03	3.93 ± 0.11	3.98 ± 0.06
IEC / meq. g^{-1})	0.77	0.81	1.92	1.84	1.32 ± 0.002	1.31 ± 0.01
L / μm	251.7 ± 1.3	267 ± 0.9	258.5 ± 1.7	254	538.5 ± 4	530 ± 2.3

796 Abbreviations: R_A – Area resistance; R_S – Specific resistance; σ - Ionic conductivity; IEC – Ion exchange capacity; L –Thickness

797

798 **Fig. 1**

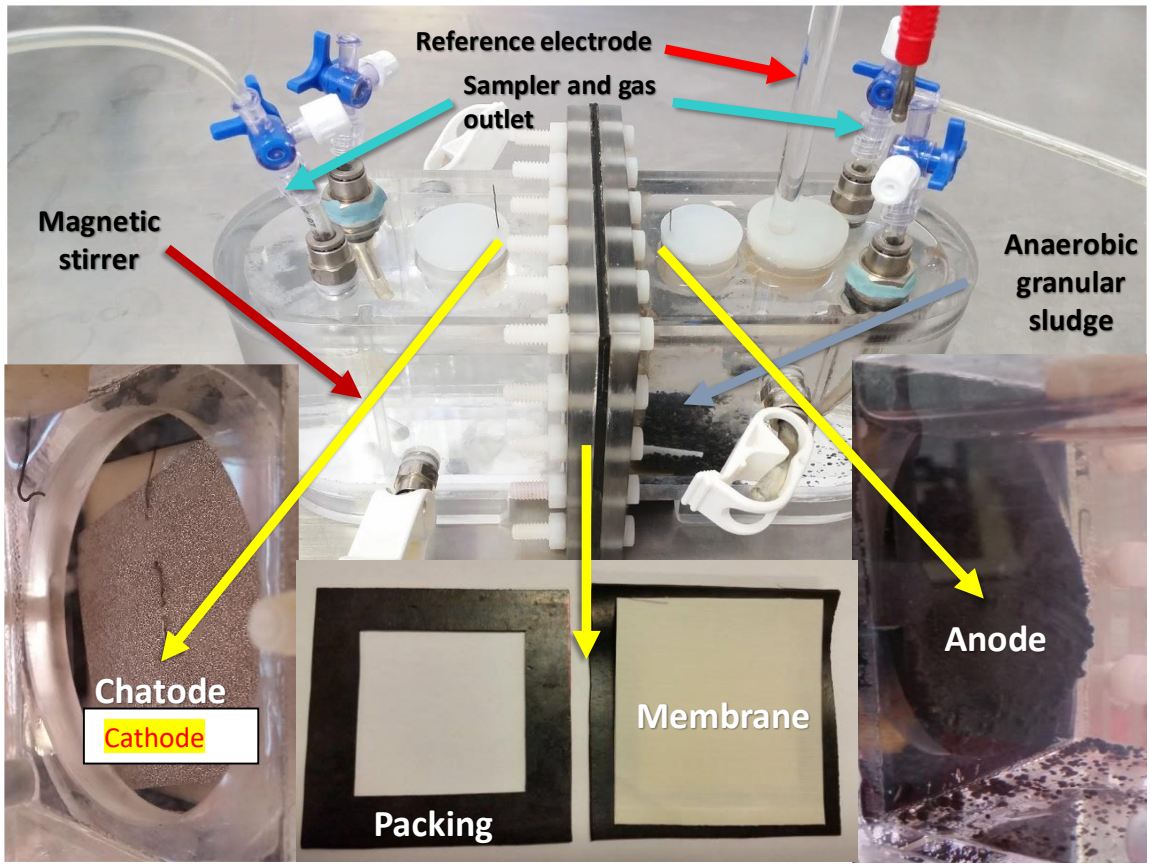

799

800

801 **Fig. 2**

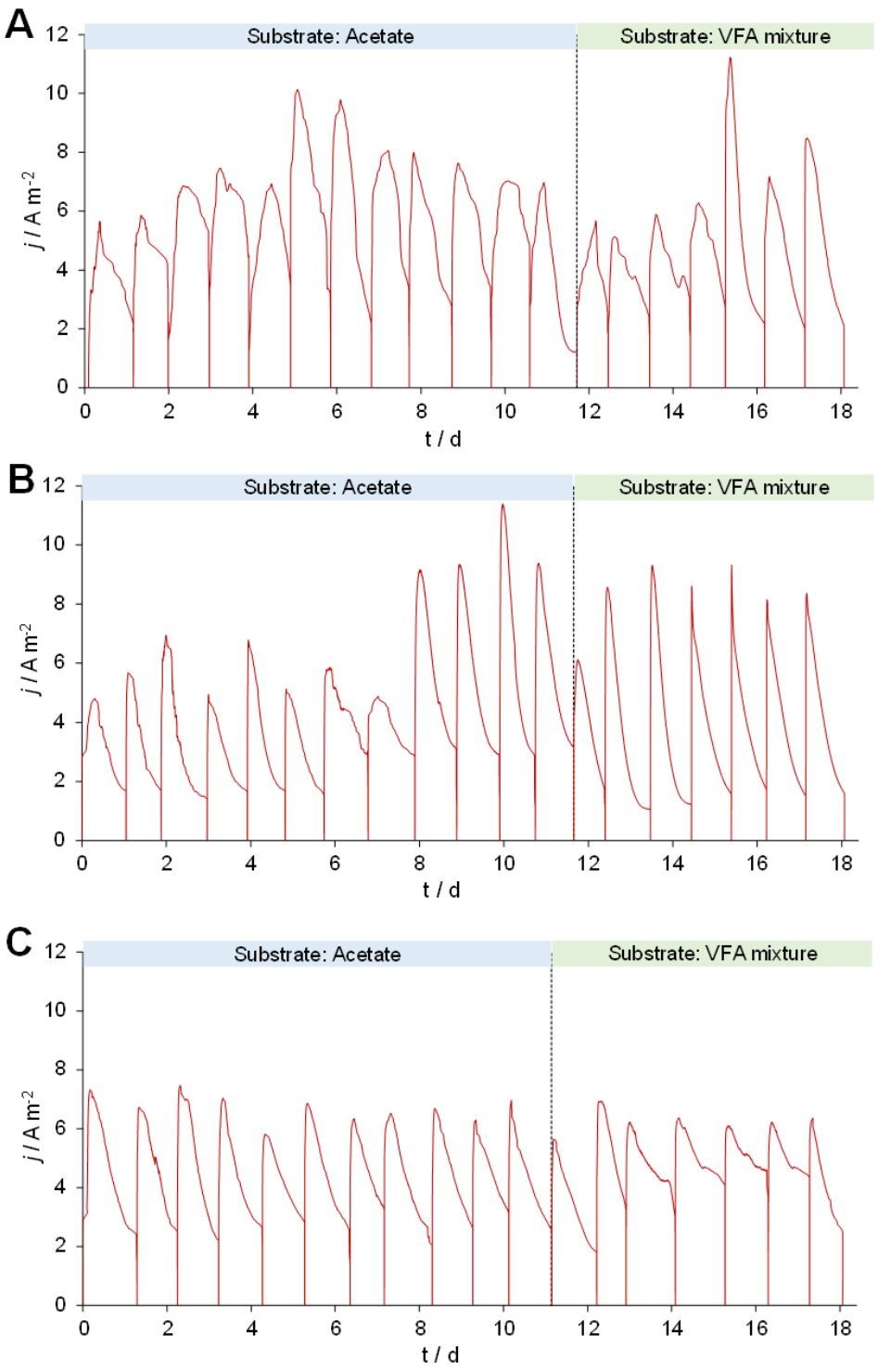

802

803

804 **Fig. 3**

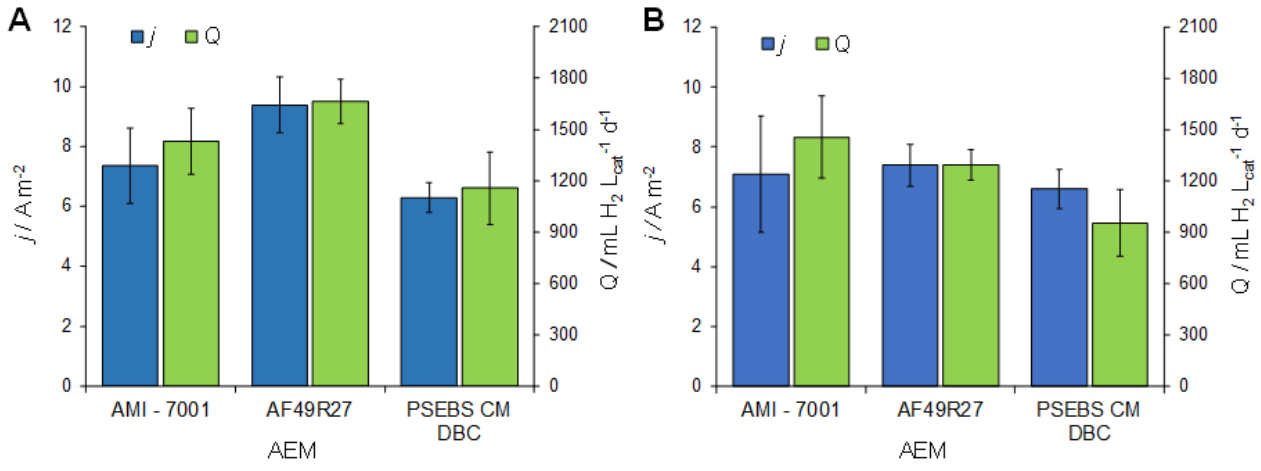

805

806

807 **Fig. 4**

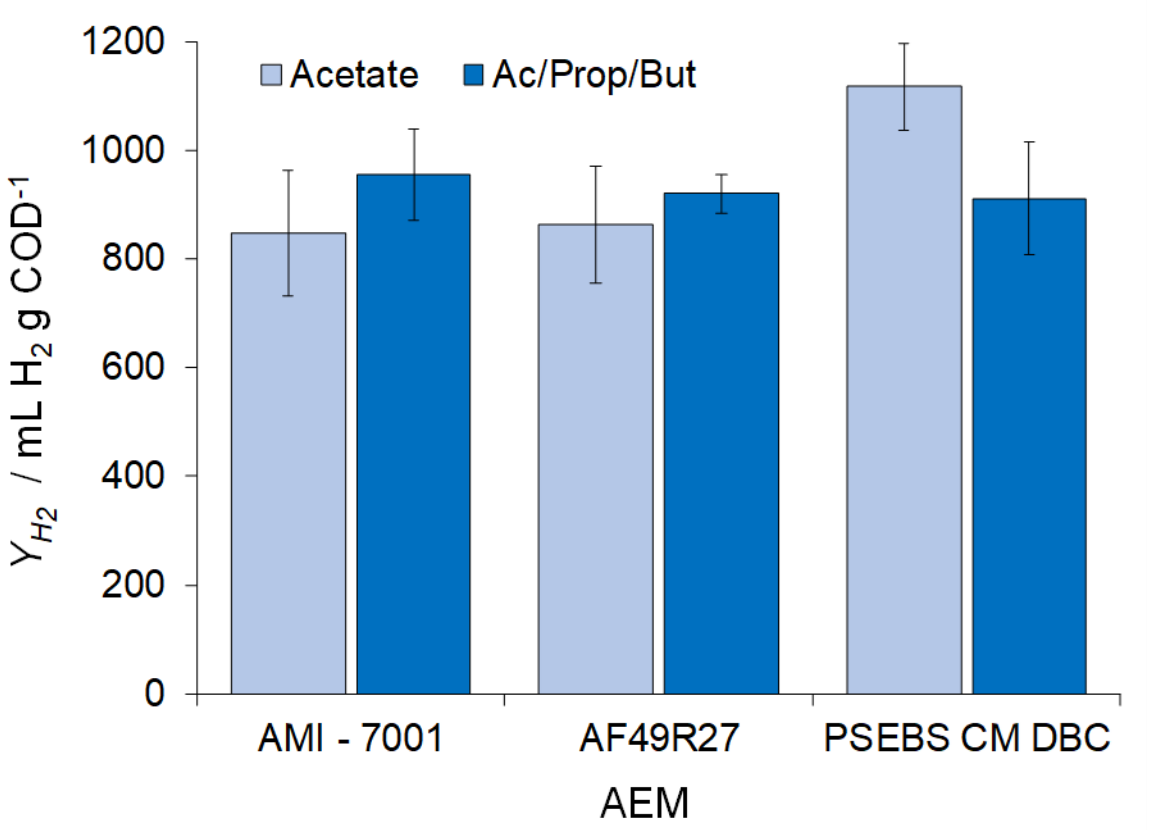

808

809

Fig. 5

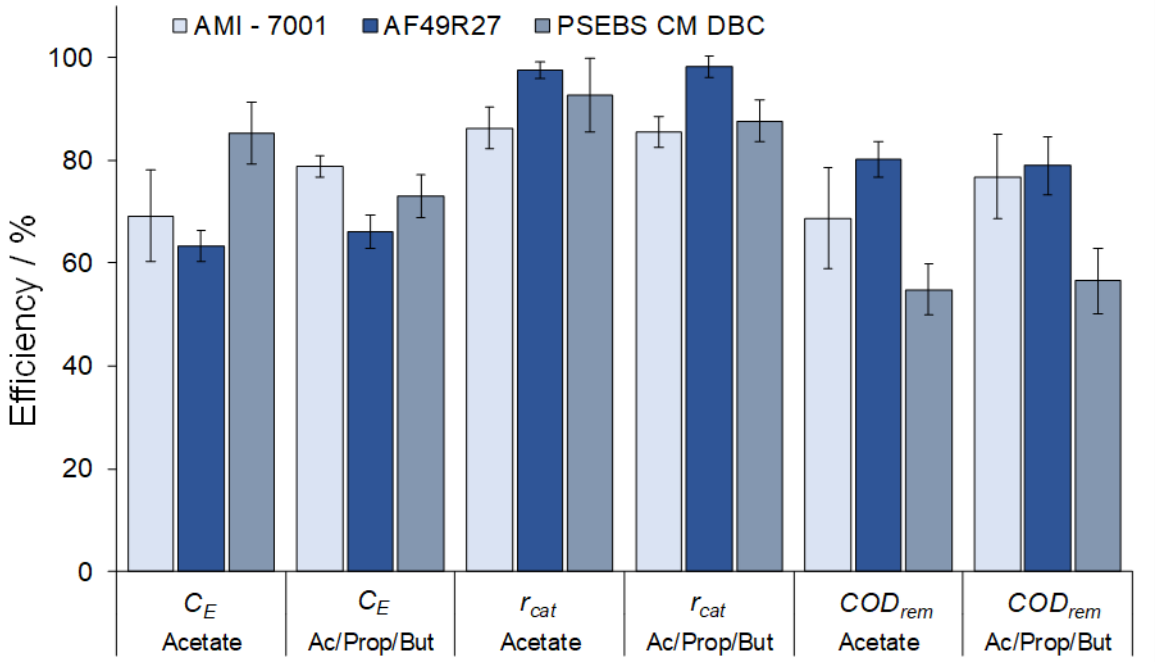
AMI - 7001
AF49R27
PSEBS CM DBC
Efficiency / %
100
80
60
40
20
0
C_E Acetate
C_E Ac/Prop/But
r_{cat} Acetate
r_{cat} Ac/Prop/But
COD_{rem} Acetate
COD_{rem} Ac/Prop/But

Fig. 6

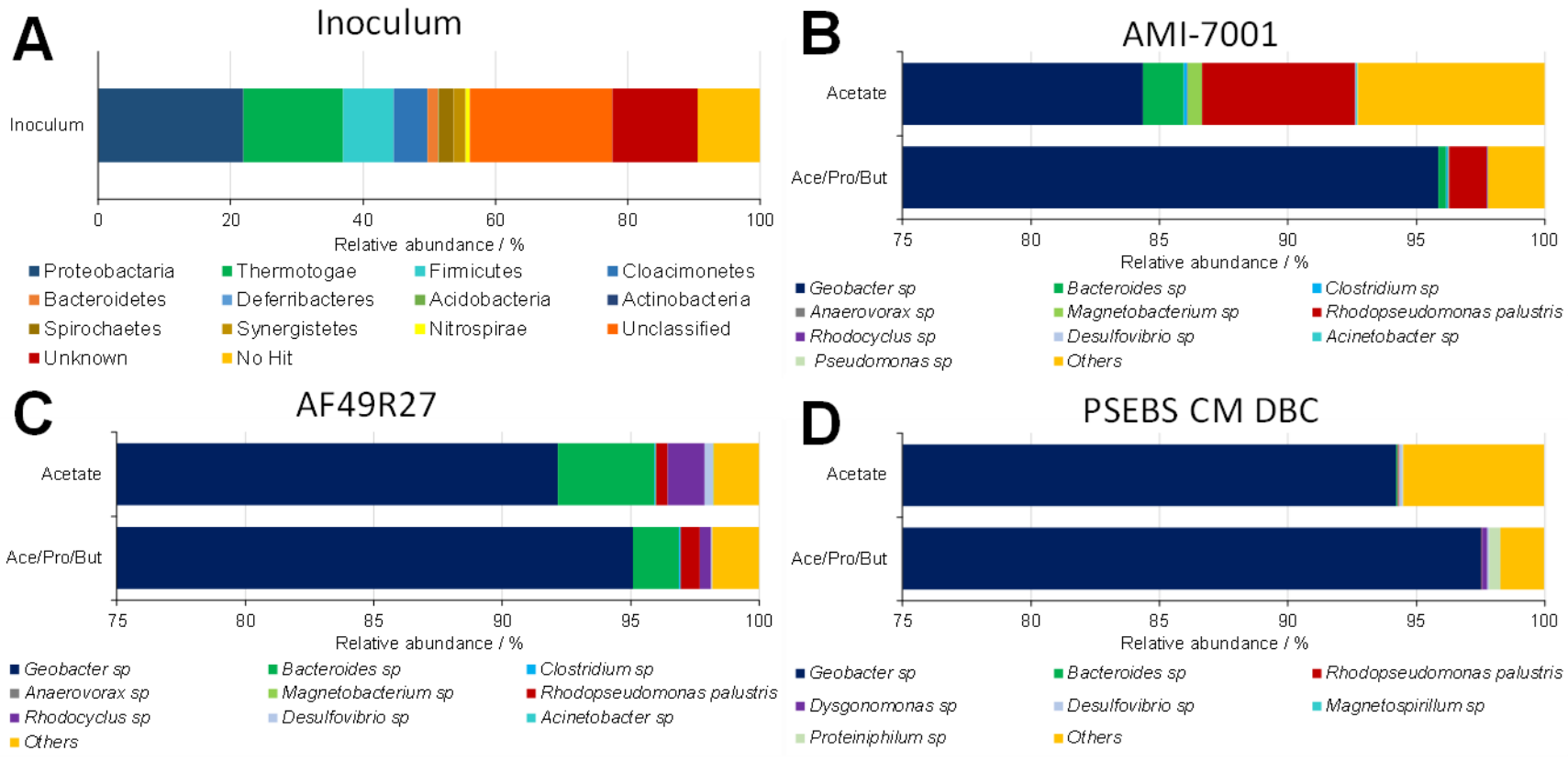
A
Inoculum
Inoculum
0
20
40
60
80
100
Relative abundance / %
Proteobactaria
Thermotogae
Firmicutes
Cloacimonetes
Bacteroidetes
Deferribacteres
Acidobacteria
Actinobacteria
Spirochaetes
Synergistetes
Nitrospirae
Unclassified
Unknown
No Hit
B
AMI-7001
Acetate
Ace/Pro/But
75
80
85
90
95
100
Relative abundance / %
Geobacter sp
Bacteroides sp
Clostridium sp
Anaerovorax sp
Magnetobacterium sp
Rhodopseudomonas palustris
Rhodocyclus sp
Desulfovibrio sp
Acinetobacter sp
Pseudomonas sp
Others
C
AF49R27
Acetate
Ace/Pro/But
75
80
85
90
95
100
Relative abundance / %
Geobacter sp
Bacteroides sp
Clostridium sp
Anaerovorax sp
Magnetobacterium sp
Rhodopseudomonas palustris
Rhodocyclus sp
Desulfovibrio sp
Acinetobacter sp
Others
D
PSEBS CM DBC
Acetate
Ace/Pro/But
75
80
85
90
95
100
Relative abundance / %
Geobacter sp
Bacteroides sp
Rhodopseudomonas palustris
Dysgonomonas sp
Desulfovibrio sp
Magnetospirillum sp
Proteiniphilum sp
Others

816 **Fig. 7**

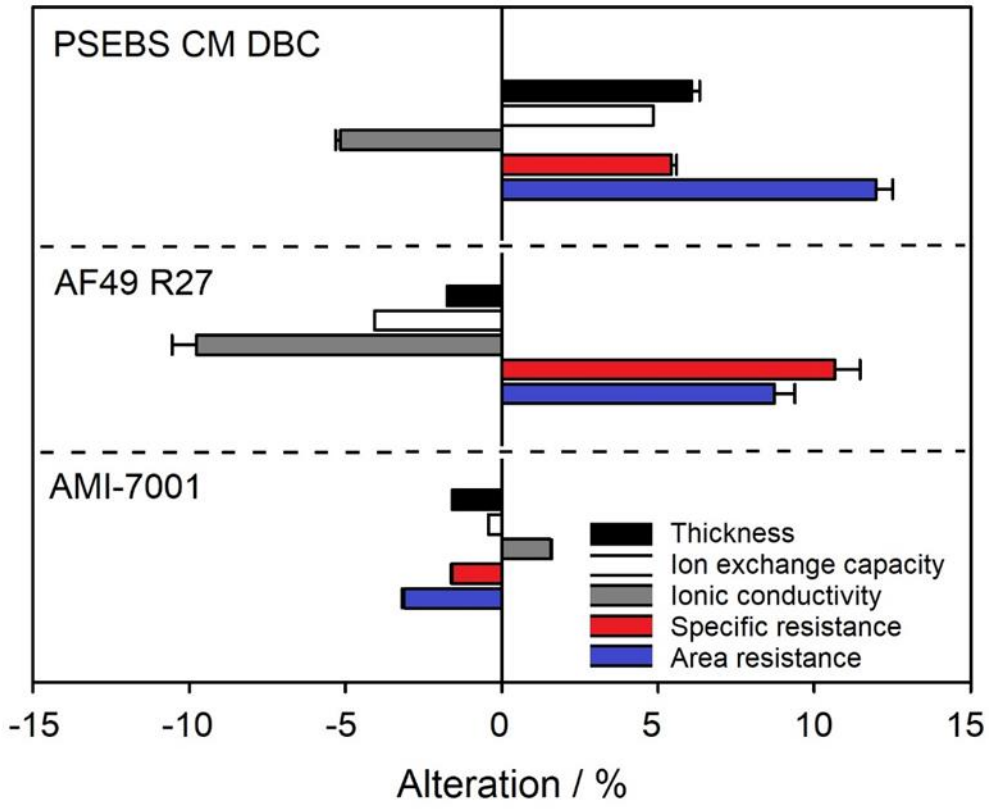
PSEBS CM DBC
AF49 R27
AMI-7001
Thickness
Ion exchange capacity
Ionic conductivity
Specific resistance
Area resistance
-15
-10
-5
0
5
10
15
Alteration / %

817